

Localization of Dual Accessory Pathways Using Two Equivalent Dipoles

Vojko Jazbinšek¹, Rok Hren¹, Gerhard Stroink^{2,3,4}, B. Milan Horáček^{3,4} and Zvonko Trontelj¹

¹Institute of Mathematics, Physics, and Mechanics, University of Ljubljana, Ljubljana, Slovenia;

²Department of Physics, ³Department of Physiology & Biophysics, ⁴School of Biomedical Engineering, Dalhousie University, Halifax, Canada

Abstract

In this study, we demonstrated that electrocardiographic and magnetocardiographic inverse solutions using a pair of equivalent dipoles could be employed in localizing dual accessory pathways. We used an anatomical computer model of the human ventricles to simulate body surface potentials and magnetic field for 8 pairs of preexcitation sites positioned on the epicardial surface along the atrio-ventricular ring. Average localization errors were in the range of 5 to 21 mm and 3 mm to 20 mm for the electrocardiographic and magnetocardiographic localizations, respectively. Such an approach could be potentially useful in pre-interventional planning of the ablative treatment

1 Introduction

Body-surface potential maps (BSPMs) and magnetic field maps (MFMs) can be reconstructed from noninvasive procedures that involve recording of multiple electrocardiograms and multiple magnetocardiograms, respectively. BSPMs and MFMs have been used to localize preexcitation sites in patients with Wolff-Parkinson-White (WPW) syndrome [1,2], where such a localization is performed by calculating the position of an equivalent single dipole source in the model of a human torso. However, the single-dipole equivalent generator is an adequate approximation only when the bioelectric activity of the heart is confined to a single very small volume. Thus, in cases where more than one preexcitation site is present, more complex equivalent generators (including two or more equivalent dipoles) would achieve better accuracy, and, therefore, a better understanding of the underlying cardiac process.

In this study, we employ an anatomical computer model to test the hypothesis that dual preexcitation sites can be localized using BSPMs and MFMs in combination with the mathematical inverse solution. The choice of the computer simulations as the methodology is supported by their ability to explore capabilities of the inverse solution systematically and under controlled conditions.

2 Methods

We used an anatomical model of the human ventricles and a homogeneous model of the human torso to simulate activation sequences and corresponding 117-lead BSPMs (covering the anterior and posterior

torso) and 64-lead MFMs (above the anterior torso) [3]. We initiated activation sequences at 10 single pacing sites located along right lateral (RL), left lateral (LL), and right/left anteroparaseptal (RAP/LAP) aspects of the atrio-ventricular (AV) ring of the epicardium (see **Fig. 1** and **Table 1**). For each activation sequence, we simulated BSPMs and MFMs at 4-ms increments within the first 40 ms after the activation onset. Next, we simulated the sequences initiated at 8 different pairs of sites in the same segments of the AV ring (**Fig. 1** and **Table 1**). To simulate measur-

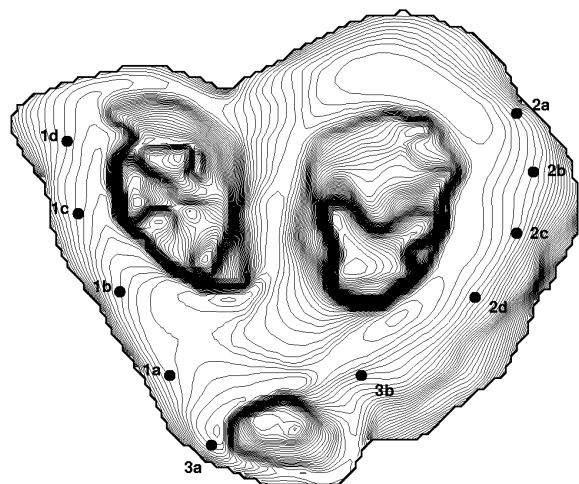


Fig. 1 Basal view of the human ventricular model shown with 10 preexcitation sites. Layers are 1 mm apart, and each is represented by smoothed contour lines to achieve better rendering of the shape. This display illustrates the amount of detail included in the reconstruction of the human ventricular model. Right ventricle is to the left, left ventricle is to the right, and pulmonary artery is to the bottom.

ing conditions, Gaussian noise at the root-mean-square (RMS) levels of 2.5 μV , 5 μV and 20 μV was added to all simulated BSPMs, and 30 fT, 120 fT and 300 fT was added to all simulated MFMs. We generated 10 different noise distributions for each noise level.

Using simulated BSPMs and MFMs as the input data, we performed the inverse solution for a pair of dipole sources in the torso model. For determining the best initial estimates, we calculated dipole moments from several randomly selected starting dipole positions around the AV ring. The final solution was then obtained with Levenberg-Marquardt least-squares fitting algorithm [4,5]. As a measure of accuracy of the localization, we used localization errors, defined as distances between locations of the best-fitting pair of dipoles and a pair of preexcitation sites in the ventricular model. We rejected all solutions for which the magnitude of the stronger of the two dipoles exceeded the weaker dipole by the factor of 5.

To account for the influence of the torso's outer boundary on electric potentials, we used an individualized male torso model [6] in simulating BSPMs and MFMs as generated by the ventricular model. Two-dipole inverse solutions were carried out using the "standard" male torso model.

For all inverse solutions, positions of reconstructed dipoles were superimposed on a realistic three-dimensional epicardial surface (that completely encloses the ventricular model) for visual inspection.

3 Results and Discussion

Macchi et al. [7] and Taccardi et al. [8] pointed out that electric potentials during the initial phase of activation resemble those of two opposing dipoles oriented along the major axis and located near the ends

Table 1 Anatomical description of dual preexcitation sites.

	Abbr.	Anat. Description	Dist.*
1a-1b	RAL	right anterolateral	18 mm
1a-1c	RAL/RL	right anterolateral/ right lateral	34 mm
1a-1d	RAL/RPL	right anterolateral/ right posterolateral	48 mm
2a-2b	LPL/LL	left posterolateral/ left lateral	11 mm
2a-2c	LPL/LL	left posterolateral/ left lateral	23 mm
2a-2d	LPL/LAL	left posterolateral/ left anterolateral	36 mm
3a-3b	RAP/LAP	right anteroparaseptal/ left anteroparaseptal	30 mm
1b-2b	RAL/LPL	right anterolateral/ left posterolateral	139 mm

*Distance measured along the AV ring.

of an elliptical wavefront of propagated activation. To test this hypothesis, we first assessed the performance of a two-dipole generator in localizing single accessory pathways. **Fig. 2** shows a typical example for localization of a single accessory pathway when using the two-dipole model under ideal (i.e., noise-free) conditions. Localization of a pair of dipoles is shown at different time instants for an activation sequence initiated at the LL site (**2c**) when using BSPMs and MFMs. Both reconstructed dipoles are initially in the sequence located close to the site of an accessory pathway, but later become separated by the distance that is progressively increasing with time. The distance between the leading edge of the simulated wavefront and locations of the two corresponding reconstructed dipoles is during the first 28 ms of an activation sequence on average 3 mm (range 1-5 mm). This observation strongly supports the notion that progressive separation of the two dipoles reflects the propagation of an activation wavefront.

Fig. 3 illustrates localization results based on BSPMs and MFMs for the pair of RAL/RL accessory pathways (case **1a-1c**). One can see that dipoles are clearly separated and located close to the actual locations of accessory pathways. In this specific case, the localization errors attained a minimum at 20 ms after the onset of activation (11 \pm 1 mm and 5 \pm 1 mm for BSPMs and 9 \pm 2 mm and 6 \pm 1 mm for MFMs).

Table 2 summarize the localization results for typical measuring conditions (RMS noise level of 5 μV and 120 fT). We found that two-dipole localization reached minimum between 12 ms and 24 ms after the onset of activation. The average localization errors were between 5 and 21 mm (12 \pm 6/11 \pm 6 mm at 20 ms for the first/second dipole, respectively) for the BSPMs and between 3 and 20 mm (11 \pm 5/12 \pm 9 mm at 24 ms) for the MFMs. Localization errors were on

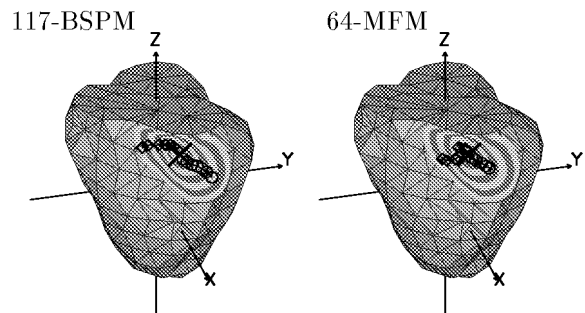


Fig. 2 Localization results for a LL single accessory pathway using a two-dipole model at different time instants (4 to 28 ms after the onset) superimposed on the epicardial surface. The onset of accessory pathway is marked by \times ; reconstructed positions are indicated as "circle" and "diamond" for the first and the second dipole, respectively. Alternating light and dark gray zones represent projection of activation isochrone surface on the epicardial surface between 4 and 28 ms after the onset of activation

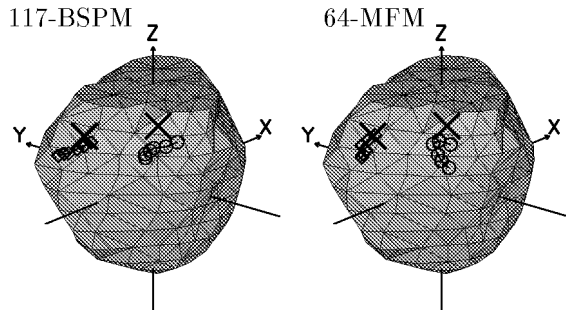


Fig. 3 Localization results for a RAL/RL dual accessory at different time instants (from 16 to 36 ms after the onset).

average smaller for the pairs of accessory pathways located on the right side (cases **1a-1b**, **1a-1c**, **1a-1d**) than for those located on the left side (cases **2a-2b**, **2a-2c**, **2a-2d**); they were 8 mm versus 14 mm for the BSPMs and 7 mm versus 11 mm for the MFMs. RMS levels of simulated BSPMs were, at 20 ms after the onset of activation, between 104 μ V (case **2a-2b**) and 164 μ V (case **1a-1c**); RMS levels of simulated MFMs were at the same time instant between 0.9 pT (case **2a-2b**) and 6.8 pT (case **1a-1d**).

When including magnetic leads near the anterior and posterior torso (in total 128 sites) to provide a lead arrangement equivalent to that of the potentials, the average localization errors slightly improved and were in the presence of RMS noise of 120 fT between 2 and 14 mm ($10 \pm 5/8 \pm 6$ mm at 20 ms).

Range of localization errors degraded to 8-22 mm ($18 \pm 8/18 \pm 9$ mm at 28 ms) for BSPMs at 20 μ V noise level, and to 3-26 mm ($14 \pm 8/15 \pm 11$ mm at 24 ms) for 64-lead and to 4-17 mm ($12 \pm 8/10 \pm 6$ mm at 24 ms) for 128-lead MFMs at 300 fT noise level.

Localization errors due to inaccuracies in rendering individualized torso boundaries (i.e., in the presence of modeling errors) reached their minimum between 16 and 28 ms after the onset. The errors were on average in the range of 11 to 39 mm ($24 \pm 18/30 \pm 13$ mm at 20 ms) for the BSPMs and of 12 to 36 mm ($20 \pm 13/29 \pm 14$ mm at 20 ms) for the MFMs. Visual inspection of inversely calculated dipole positions revealed that they were often distal to the actual locations of accessory pathways and sometimes fell out of anatomically plausible region.

Results of our study suggest that the magnetocardiographic inverse solution is at least as accurate as electrocardiographic inverse solution when using a two-dipole model.

4 Acknowledgements

This work was supported by the Ministry of Education, Science, and Sport, Republic of Slovenia and the Natural Sciences and Engineering Research Foundation (NSERC) of Canada.

Table 2 Localization accuracy for 117-lead BSPMs (noise 5 μ V) and 64-lead anterior MFM (120 fT).

	117 BSPM (5 μ V)	64 MFM (120 fT)
1a-1b	9 \pm 3 / 7 \pm 3 (16 ms)*	7 \pm 3 / 7 \pm 3 (20 ms)
1a-1c	11 \pm 1 / 5 \pm 1 (20 ms)	9 \pm 2 / 6 \pm 1 (20 ms)
1a-1d	11 \pm 6 / 5 \pm 1 (12 ms)	10 \pm 2 / 3 \pm 1 (24 ms)
2a-2b	21 \pm 10 / 11 \pm 4 (24 ms)	12 \pm 8 / 9 \pm 5 (24 ms)
2a-2c	19 \pm 12 / 8 \pm 6 (20 ms)	12 \pm 3 / 9 \pm 4 (24 ms)
2a-2d	14 \pm 9 / 13 \pm 5 (16 ms)	14 \pm 7 / 10 \pm 4 (24 ms)
1b-2b	7 \pm 2 / 8 \pm 3 (16 ms)	4 \pm 2 / 20 \pm 7 (16 ms)
3a-3b	11 \pm 2 / 10 \pm 6 (20 ms)	11 \pm 4 / 13 \pm 18 (20 ms)
Total	12 \pm 6 / 11 \pm 6 (20 ms)	11 \pm 5 / 12 \pm 9 (24 ms)

*Time after the onset of activation when localization error attained minimum for a given site.

5 Literature

- [1] Savard, P.; Ackaoui, A.; Gulrajani, R.M.; Nadeau, R.; Roberge, F.A.; Guardo, R.; Dube, B.: Localization of cardiac ectopic activity in man by a single moving dipole. Comparison of different computation techniques. *J. Electrocardiol.* 18 (1985), 211-222
- [2] Nenonen, J.; Purcell, C.J.; Horáček, B.M.; Stroink, G.; Katila, T.: Magnetocardiographic functional localization using a current dipole in a realistic torso. *IEEE Trans. Biomed. Eng.* 38(1991), 658-664
- [3] Hren, R.; Horacek, B.M.: Value of simulated body surface potential maps as templates in localizing sites of ectopic activation for radiofrequency ablation. *Physiol. Measur.* 18 (1997), 373-400
- [4] Hren, R.; Stroink, G.; Horacek, B.M.: Accuracy of the single dipole inverse solution in localizing ventricular preexcitation sites: a simulation study. *Med. Biol. Eng. Comp.* 36 (1998), 323-329
- [5] Jazbinsek, V.; Hren, R.: Influence of randomly displaced BSPM leads on the identification of ventricular preexcitation sites. *Biomed. Techn.* 44 Suppl. 2 (1999), 104-107
- [6] Hren, R.; Stroink, G.; Horacek, B.M.: Spatial resolution of body surface potential maps and magnetic field maps: a simulation study applied to the identification of ventricular preexcitation sites. *Med. Biol. Eng. Comp.* 36(1998), 145-157
- [7] Macchi, E.; Arisi, G.; Taccardi, B.: Identification of ectopic ventricular foci by means of intracavitary potential mapping: a proposed method. *Acta Cardiol* 47 (1992), 421-433
- [8] Taccardi, B.; Macchi, E.; Lux, R.L.; Ershler, P.R.; Spaggiari, S.; Baruffi S; Vyhmeister, Y.: Effect of myocardial fiber direction on epicardial potentials. *Circulation* 90 (1994), 3076-3090.